

Nanocrystal Film Patterning by Inhibiting Cation Exchange via Electron-Beam or X-ray Lithography

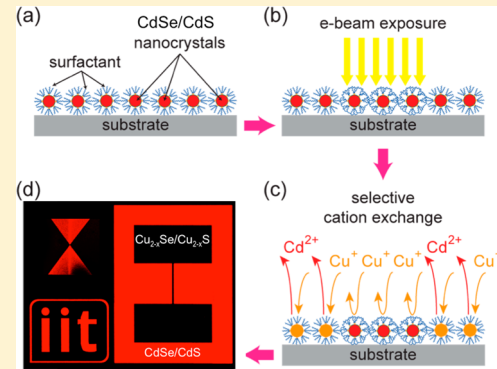
Karol Miszta, Fanny Greullet, Sergio Marras, Mirko Prato, Andrea Toma, Milena Arciniegas, Liberato Manna,* and Roman Krahne*

Istituto Italiano di Tecnologia, Via Morego 30, 16163 Genova, Italy

Supporting Information

ABSTRACT: In this Letter we report patterning of colloidal nanocrystal films that combines direct e-beam (electron beam) writing with cation exchange. The e-beam irradiation causes cross-linking of the ligand molecules present at the nanocrystal surface, and the cross-linked molecules act as a mask for further processing. Consequently, in the following step of cation exchange, which is performed by directly dipping the substrate in a solution containing the new cations, the regions that have not been exposed to the electron beam are chemically transformed, while the exposed ones remain unchanged. This selective protection allows the design of patterns that are formed by chemically different nanocrystals, yet in a homogeneous nanocrystal film. Spatially resolved compositional analysis by energy-dispersive X-ray spectroscopy (EDS) corroborates that the selective exchange occurs only in the nonirradiated regions. We demonstrate the utility of this lithography approach by fabricating conductive wires and luminescent patterns in CdSe/CdS nanocrystal films by converting nonirradiated regions to Cu_{2-x}Se/Cu_{2-x}S. Furthermore, we show that X-ray irradiation too can lead to protection from cation exchange.

KEYWORDS: Cation exchange, electron-beam lithography, nanocrystal films, X-rays, electrical circuits



Colloidal inorganic nanocrystals (NCs) are among the most exploited nanomaterials due to their extreme versatility.¹ They are synthesized directly in the liquid phase and couple the advantage of being made of a core of one or more inorganic materials, which guarantees their structural stability and resistance to degradation, with the additional feature of being coated with a monolayer shell of organic passivating ligands. The ligands passivation of the surface ensures their solubility in a variety of solvents and is at the basis of their ease of processability, as if they were standard macromolecules. An additional step forward in NC research was the creation of a wide range of superstructures from the assembly of such NCs, which can be thought of as new types of artificial solids.^{2–6} This, coupled with the possibility to replace the native ligands on the surface of the NCs with shorter molecules, down to single atom ligands, has conferred unique optical and electrical features to films of NCs that make them attractive for low cost alternatives to many technologies in photovoltaics, optics, and electronics.^{7–11} Hand in hand with advances in surface ligand exchange, methods for the fabrication of homogeneous NC films with good thickness control have been developed, for example employing layer-by-layer processes^{3,12} in which each step of deposition of lead–chalcogenide NCs was followed by a change of the polarity of the surface through ligand exchange to avoid NC redissolution on successive layer deposition.

Several efforts have been made to create patterned NC films, for example via controlled dewetting of a NC solution¹³ or by selective deposition of NCs into etched trenches on a substrate by exploiting capillary forces.¹⁴ A variety of printing methods have been exploited for precise patterning of NCs, for example, dip pen lithography,^{15,16} doctor-blading,¹⁷ and inkjet printing.^{18,19} Most of these printing approaches require several processing steps: either the substrate has to be functionalized prior to NC deposition, or a polymer resist layer is involved in the patterning of arbitrary designs, followed by a lift-off step.²⁰ Electron beam irradiation has been used also to directly write motifs on films of nanoparticles:^{21–24} in that case, irradiation modified the structure of the ligands on the NC surface, leading to ligand polymerization.^{25–27} As a result, the irradiated NCs were anchored to the substrate and linked to each other, while particles in the nonirradiated regions remained unaffected and could be removed. Loss of orientational and conformational order, cleavage of C–H bonds, and partial dehydrogenation leading to carbon double bond formation, as well as desorption of layer fragments, have been reported as the processes caused by the electron-beam irradiation of linear alkanes.^{22,28} Also, the irradiation-induced effects were found to be essentially

Received: January 28, 2014

Revised: March 4, 2014

Published: March 4, 2014

independent of the alkyl chain length and of the substrate material.²⁸

Recently, exciting new directions in the field of colloidal NCs have been unveiled by studying chemical transformations in nanostructures, most notably via cation exchange,^{29–36} which involves replacement of the sublattice of cations in a crystal with a new sublattice of different cations, while the sublattice of anions remains in place. Pioneering work on mastering exchange on several types of particles has greatly expanded the collection of nanomaterials that can now be prepared and that otherwise would be inaccessible by direct chemical synthesis or by other means of fabrication.^{30,31,37} This is due to the evidence that during cation substitution in NCs the framework of anions remains stable even in more elaborate structures; thus the overall shape of the NCs was usually preserved. If appropriate protocols are followed, any residual cations from the starting NCs can be removed, so that in principle the exchanged NCs are suitable for optoelectronic applications.³³ Also, partial replacement of the original cations has been successfully exploited to create segmented or even striped nanostructures.^{34,35,38} In some cases, these reactions can even yield NCs characterized by a crystal structure that is metastable in the bulk or that does not even exist in their bulk counterpart.³⁶ Furthermore, a recent work has shown that coating of colloidal CdSe-based NCs with polymer shells with different permeability can be exploited to allow or to block cation exchange reactions.³⁹

In this work we demonstrate an approach for NC film patterning by locally inhibiting the cation exchange reaction via the exposure of the film to an electron beam or to an X-ray beam, as illustrated in Figure 1. NCs coated by native ligand molecules are homogeneously deposited on a substrate, as depicted in Figure 1a. The direct exposure of the NC film to the high energy beam results in a cross-linking of the organic

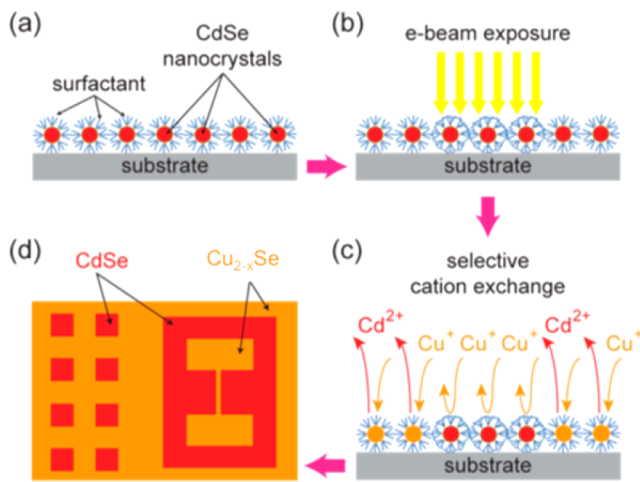


Figure 1. Sketch of the masked cation exchange process: (a) Cross section of a thin film consisting of NCs that are coated on their surface with organic surfactant molecules. (b) Selected regions of the NC film are exposed to an e-beam that cross-links the surfactant molecules. (c) Cation exchange occurs only in regions that had not been exposed to the e-beam. (d) Top view of possible patterns consisting of two chemically different NCs, for example, Cu_{2-x}Se and CdSe, within the previously homogeneous film. The different optical and electrical properties of the two materials can be exploited to obtain patterned light emitting regions (square array on the left) or electrically conducting circuits (pads connected by a wire on the right).

ligand molecules passivating the NC surface (Figure 1b), which prevents the flow of cations in the following cation exchange reaction (Figure 1c). Consequently, our method yields patterns of chemically different NCs within a homogeneous NC film, as sketched in Figure 1d, and the range of possible NC material combinations in the film is defined by the cation exchange process. To demonstrate the versatility of our masked cation exchange lithography technique, we chose the room temperature $\text{Cd} \rightarrow \text{Cu}$ exchange route. Nanocrystals of Cd-based chalcogenides are among the most studied NC materials and therefore are excellent candidates to explore novel processes. Starting from NCs of materials such as CdSe and CdS, these can be easily transformed to Cu_{2-x}Se and Cu_{2-x}S , respectively, via cation exchange.^{40,41} Furthermore, since the anion sublattice remains stable during the process, the exchange works also for core–shell architectures, like CdSe(core)/CdS (shell) NCs,^{32,41} transforming them to $\text{Cu}_{2-x}\text{Se}(\text{core})/\text{Cu}_{2-x}\text{S}(\text{shell})$ NCs.

In this work we used CdSe, CdS, and core–shell CdSe/CdS NCs as starting materials, which were dispersed in toluene and stabilized by native surface ligands (see synthesis section in Supporting Information (SI)) on their surface. We deposited a homogeneous NC film on a substrate, for example by spin coating or via layer-by-layer deposition.⁴² The NC films shown in Figure 2a, with thickness of few monolayers, were spin-coated from a toluene solution onto Si/SiO₂ substrates. In detail, 15 μL of NC solution at a concentration of 2 μM was deposited on previously cleaned Si/SiO₂ substrates, already mounted in the spin coater, and after 2 min the sample was spun at 2500 rpm for 4 min. The uniformity of the obtained NC films even over large areas is clearly seen in Figure S1 of the SI. In the next step, the NC films were exposed to an electron-beam using a Raith 150-two lithography system, with an acceleration voltage of 10 kV and an exposure dose in the range of 0.1–20 mC/cm².

Cation exchange on the NC films was performed by immersion of the samples in 5 mL of a solution of a Cu(I) complex (namely, Cu(I) tetrakis (acetonitrile) hexafluorophosphate) in methanol (60 mg/mL) for 45 min. An excess of copper complex was used to ensure full replacement of the cations in the unexposed areas of the NC films (the amount of Cu(I) in the solution exceeded the amount of Cd atoms in the film by several orders of magnitude). After exchange, the samples were immersed in methanol twice, for 30 min each, to remove excess copper/cadmium species from the surface of the film.

In the following, we focus on CdSe/CdS NCs that were converted to $\text{Cu}_{2-x}\text{Se}/\text{Cu}_{2-x}\text{S}$ (see Figure 2a) following published procedures.^{32,38,41} This material system has the advantage that the CdSe/CdS NCs have a bright photoluminescence (PL) in the visible region^{43,44} that can be easily detected via confocal imaging⁴⁵ while $\text{Cu}_{2-x}\text{Se}/\text{Cu}_{2-x}\text{S}$ NCs are not emitting in this spectral range. Therefore spatial imaging of the PL is a convenient and noninvasive tool to reveal the NC transformation in the film. Furthermore, $\text{Cu}_{2-x}\text{Se}/\text{Cu}_{2-x}\text{S}$ NC films had an appreciable conductivity, while the CdSe/CdS NC films were not conducting current within our detection limit of 1 pA (this is true for NC coated with their native surfactants, which are mainly alkyl phosphonic acids). Therefore this material combination allows the realization of conductive circuits in the NC film, as will be demonstrated later.

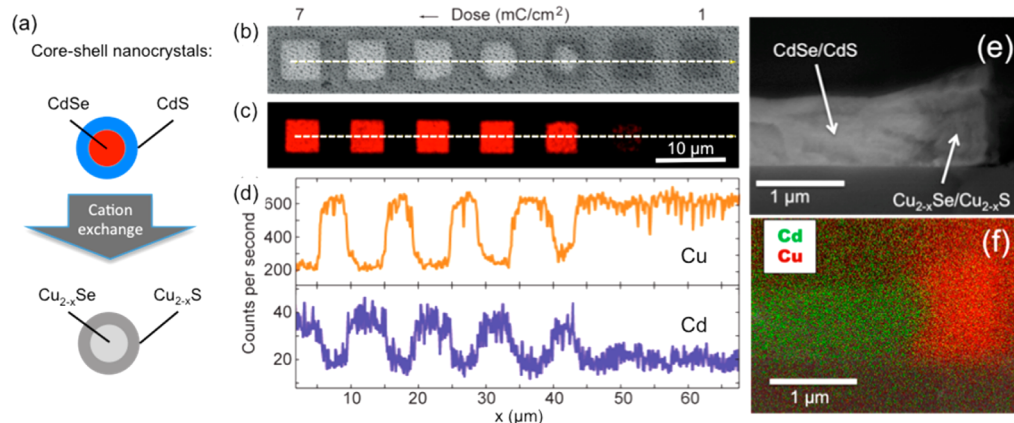


Figure 2. (a) Illustration of core–shell NC architecture before and after cation exchange. (b) BSE SEM image of a square array masked by e-beam with dose ranging from $1 \text{ mC}/\text{cm}^2$ to $7 \text{ mC}/\text{cm}^2$. (c) Corresponding confocal image recorded in the band 570 – 670 nm with a laser excitation at 405 nm . (d) Elemental analysis via EDS for Cu and Cd, following the line scan highlighted by the dashed line in (b,c). Cross section BSE SEM (e) and EDS (f) images of a relatively thick NC film that reveal the z profile of the interface between the protected and cation exchanged regions, and which demonstrate that the exposure is effective throughout the film thickness.

Figure 2b–d shows experimental data from a NC film region where a row of squares was exposed with different e-beam doses, increasing from 1 to $7 \text{ mC}/\text{cm}^2$ (from right to left). The exposed squares could be distinguished in backscattered electrons (BSE) SEM images, as shown in Figure 2b: here, regions exposed to a high e-beam dose had brighter contrast than regions exposed to a comparatively lower dose. The brighter contrast correlates with greater average Z in the CdSe/CdS regions as compared to the Cu_{2-x}Se/Cu_{2-x}S ones. The dark contrast of the squares with comparatively low exposure dose (on the right) results from carbon deposition. The absence of PL from these squares indicates that the e-beam induced modification of the surface ligands was not sufficient to prevent the cation exchange reaction. The strong PL originating from the exposed regions with high e-beam dose (Figure 2c) is an indicator of successful masking from cation exchange, since this bright emission in the visible can only originate from CdSe/CdS NCs. Additionally the wavelength of the emission from the protected regions was not affected by the process, demonstrating that the electronic structure of the NCs was not modified by the overall process (see Figure S4 in the SI). To evaluate in more detail the Cu and Cd content in the respective regions, we performed elemental analysis of the films via energy-dispersive spectroscopy (EDS) along the line scan indicated in Figure 2b,c. The results are reported in Figure 2d, where we observe a clear correlation of high Cd content with the occurrence of PL, and high Cu content in the dark regions. Figure 2e,f shows a cross section of a core–shell NC film, where the part on the left was exposed by an e-beam before cation exchange was performed. In the BSE SEM image (Figure 2e) the interface between the Cu_{2-x}Se/Cu_{2-x}S and CdSe/CdS regions can be distinguished by the change in contrast, which is darker for Cu_{2-x}Se/Cu_{2-x}S. EDS mapping for Cd and Cu confirmed the composition of the NC film, as demonstrated in Figure 2f. The protection from cation exchange extended throughout the film thickness, even for relatively thick films as shown in Figure 2e. Preliminary experiments on sequential exchange reactions from Cd²⁺ to Cu⁺ and then from Cu⁺ to Pb²⁺ on patterned NC films are reported in section 7 of the SI.

Figure 3a shows BSE SEM images of a NC film with few monolayer thickness that was patterned with a bowtie design in which the distance between the two sharp pointed triangles was

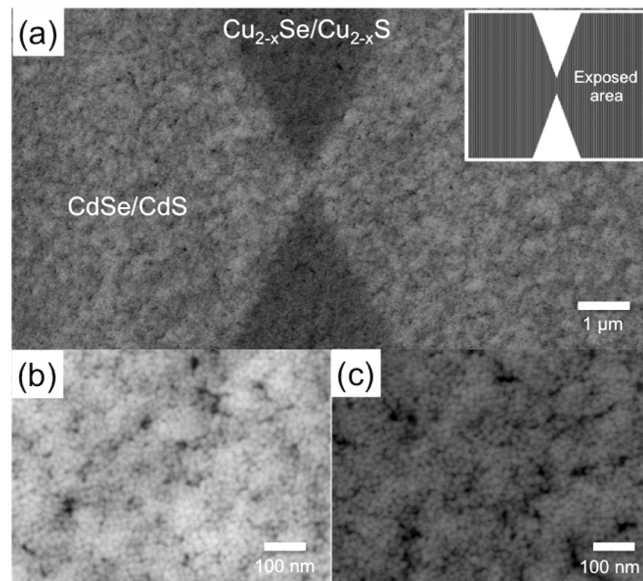


Figure 3. (a) BSE SEM images of a core–shell NC film that was patterned in a bowtie design by EBL followed by cation exchange. CdSe/CdS NC regions appear brighter due to larger average Z compared to the Cu_{2-x}Se/Cu_{2-x}S ones. The inset illustrates the pattern used for e-beam exposure. (b–c) Higher magnification of the CdSe/CdS (b) and Cu_{2-x}Se/Cu_{2-x}S (c) regions resolving individual NCs and demonstrating that the topology of the film is maintained.

set to 200 nm . From the well-distinguishable difference in Z-contrast the bowtie pattern can be easily recognized, and we estimate the fabricated distance between the two Cu_{2-x}Se/Cu_{2-x}S triangles to be around 250 – 300 nm . The ultimate limit of the masked cation exchange should be given by the NC size, and using small NCs this could be pushed ideally to around 1 nm . We can exclude fractional exchange within a single nanocrystal because, once the highly diffusive Cu⁺ ions find a channel to the inorganic NC core, this will result in replacement of the Cd²⁺ cations in the entire NC. Another limiting factor is the resolution of the irradiation process. Electron-beam lithography can achieve a resolution of sub- 10 nm when working with thin films of PMMA resist on semi-insulating substrates.⁴⁶ Here we used NCs with a 20 nm

diameter, and we estimate the resolution from the BSE SEM image in Figure 3a to be around 50–100 nm, which is only slightly larger than the one typically achieved with a PMMA resist of similar layer thickness. The high magnification BSE SEM images in Figure 3b,c that resolve individual NCs demonstrate that the NC size and shape is conserved by the processing and that the film structure remains homogeneous in the patterned regions.

To get more insight in the origin of the masking effect caused by the e-beam, we performed X-ray photoelectron spectroscopy (XPS) on our samples before and after electron beam exposure. The XPS characterization on the sample after irradiation was performed before cation exchange was done on it, to avoid signals from the organic species used in the exchange process. After irradiation, the C 1s peak position slightly shifted toward lower binding energy values, and its width at half-maximum increased (see Figure S3a in the SI). A similar effect was observed by Wu et al. on e-beam exposed self-assembled monolayers of octadecanethiol on Au²⁵ and was assigned to the cleavage of the primary C–H bonds and subsequent intra- and intermolecular cross-linking, thus affecting the hybridization state of carbon (from sp³ to sp²). To further confirm this cross-linking process, we also collected X-ray induced Auger electron spectroscopy (XAES) on the C KLL Auger line, that is known to be a better indicator of the carbon hybridization state than the XPS signal.⁴⁷ The sp²/sp³ ratio could be quantified by looking at the so-called D parameter, that is, the peak-to-peak distance between the maximum and the minimum of the first derivative of the X-ray-induced C KLL spectrum.⁴⁷ By comparing the first derivative spectra obtained from the NC films before and after e-beam exposure, as depicted in Figure S4b in the SI by the black and red lines, respectively, we observed that the D parameter increased due to e-beam exposure from 13.8 eV (± 0.4 eV, compatible with no sp² carbon in the analyzed area⁴⁸) to 15.2 eV. This second value is consistent with a sp² concentration of approximately 50%, according to the polyethylene–polystyrene copolymer calibration curve reported in refs 48 and 49.

We additionally investigated the impact of the e-beam exposure on the mechanical behavior of the films by nanoindentation, using a CSM UHNT indenter (see section 5 in the SI for details). Comparison of the P–h curves recorded from exposed and unexposed regions showed significantly increased hardness and lower penetration depth in the exposed region, as demonstrated in Figure S5. This behavior can be explained by a change in the deformation mechanism as follows: in the unexposed film the collective response of the NCs is that of a granular material, which is driven by sliding motion of the particles, similar to the model used by Lee et al.⁵⁰ Upon e-beam exposure, the deformation mechanism is similar to that of a polymer-based composite material, in which the sliding motion of the particles is inhibited by the cross-linking of the surfactant molecules of neighboring NCs.^{51,52} Therefore the increase in hardness supports cross-linking of the surfactant molecules by e-beam exposure.

We were also able to inhibit the cation exchange process by exposing the core–shell CdSe/CdS NC films to X-ray irradiation from a synchrotron radiation source (ELETTRA), schematically shown in Figure 4a. In this case we exposed circular patterns in the NC films that were defined by a metallic stencil mask to a beam with 30 kJ/cm² intensity. The successful masking of the exposed areas was verified by fluorescence microscopy and EDS mapping of Cu and Cd, as shown in

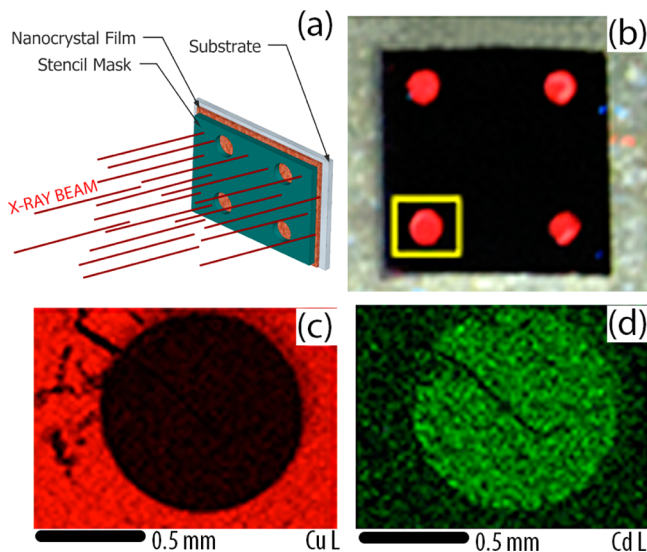


Figure 4. (a) Sketch illustrating the X-ray exposure experiment of the NC film, via a stencil mask with four circular holes, which was carried out at the DXRL beamline of the Elettra synchrotron facility. (b) Optical fluorescence image recorded under UV illumination of a NC film that was exposed to X-ray radiation with a dose of 30 kJ/cm², followed by cation exchange, as described in the text. The four red spots correspond to the layout of the stencil mask used for the exposure. (c–d) EDS maps of Cd (d) and Cu (c) acquired from the highlighted area of panel b.

Figure 4c and d. The protection of the NCs from cation exchange with X-ray evidence that the cross-linking of the surface ligands was indeed at the origin of the masking, because X-ray exposure is well-known to lead to polymerization of organic molecules^{53,54} and does not result in the deposition of a carbon layer on the surface of the sample, as e-beam exposure does.

The “masked cation exchange” approach developed by us and applied to Cd chalcogenide films can be used to create luminescent patterns in NC films as demonstrated in Figure 2c, and to fabricate electrical circuit patterns. Figure 5a shows a PL image of a NC film where two pads are connected by a straight wire with 10 μm width: here pads and wire consist of Cu_{2-x}Se/Cu_{2-x}S, whereas the surrounding material is CdSe/CdS. For these experiments, the samples were kept under air for 24 h prior to measurements (see section 8 in the SI); therefore we expect a slight decrease in Cu stoichiometry in the Cu_{2-x}Se/Cu_{2-x}S NCs.^{55–58} We performed electrical measurements under ambient conditions with a micromanipulator probe station (Suss) using tungsten micromanipulators as probes. The current was recorded with a Keithley 2612 sourcemeter. The current measured on the wire connecting the two pads is reported in Figure 5b by the solid black line, yielding Ohmic conductivity of 250 μS/cm, while the CdSe/CdS regions did not conduct any current above our detection threshold of 1 pA (see red-dashed line recorded from not-connected pads in b). Experiments on devices with different wire width and layer thickness showed that the conductance scaled linearly with the wire cross section, as reported in Figure 5c for different channel widths. The same kind of electrical circuit was obtained via masked cation exchange by e-beam from a different material system, namely, patterns of rod-shaped Cu_{2-x}S NCs obtained via masked exchange on films of CdS nanorods, as shown in Figure 5d. Here, the initial NC film was prepared by slow

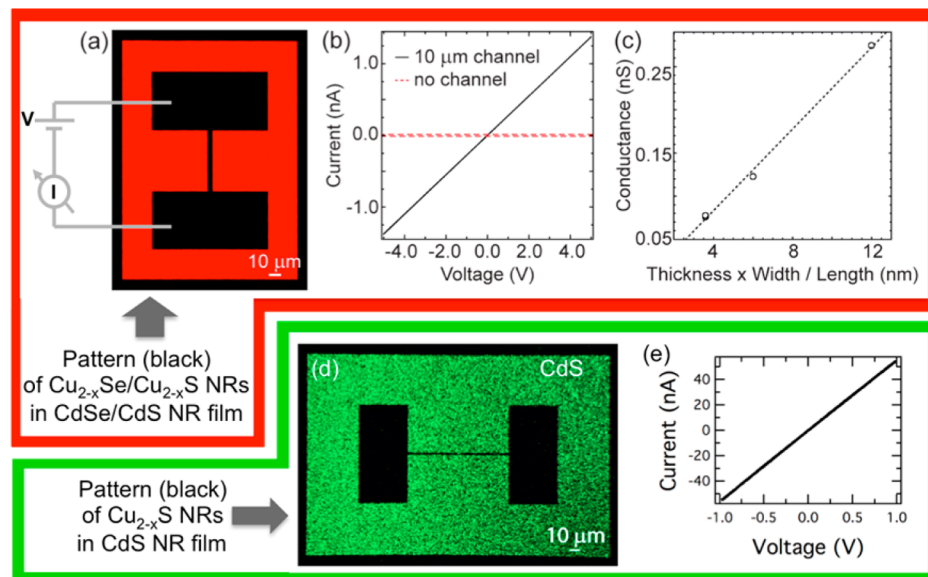


Figure 5. Electrical circuit pattern defined by the masked cation exchange process: (a) Confocal image of a two pads connected by a wire consisting of $\text{Cu}_{2-x}\text{Se}/\text{Cu}_{2-x}\text{S}$ NCs, embedded in a CdSe/CdS NC film. (b) Current–voltage (I – V) characteristics measured from two not-connected pads (red dashed line) and two connected pads (black line) as shown in a. (c) Conductance of $\text{Cu}_{2-x}\text{Se}/\text{Cu}_{2-x}\text{S}$ NC wires with different lengths and widths (film thickness of 100 nm was kept constant). The dashed line is a linear fit, which slope relates to the conductivity of the cation-exchanged NC film. (d) Confocal image of wire connecting two pads consisting of Cu_{2-x}S NCs in a CdS NC film. (e) I – V recorded from the wire displayed in d.

solvent evaporation, resulting in film thickness of around 500 nm, and the wire width and length were 2 and 100 μm , respectively. Also in this case we obtained Ohmic behavior for the wire (Figure 5e), with a conductivity of around 5 S/cm. The relatively low conductivity of the wires in Figure 5 is due to current limited by the barriers in between the individual NCs. These barriers arise from the molecules that stabilize the NC surface,^{1,59} which were oleic acid for the core–shell NCs in Figure 5a–c, and a mixture of octadecylphosphonic and hexylphosphonic acids in the case of CdS and CdSe NCs. We note that the voltage drop per NC is relatively small on the wire motifs that we measured: with 5 V on 50 μm distance and 20 nm NC diameter we obtain a voltage drop of around 2 meV per NC. The barrier imposed by alkylphosphonic acid ligands can be expected to be around some hundreds of millielectron volts,^{60,61} leading to linear behavior even at high bias. Future efforts will focus on optimizing the surface ligands for increased conductivity while maintaining efficient cross-linking capability to provide protection from cation exchange.

Apart from NCs passivated with their native ligands, we also tested the masking of the cation exchange on NC films on which the native surfactants coating the surface of the NCs (that were characterized by long alkyl chains) were replaced with hydrazine, a small molecule that does not contain carbon atoms, and which has been successfully employed by many groups to increase the film conductivity of CdSe, CdS, and PbS NC films.^{1,45,62} On these ligand-exchanged films, we found that the e-beam masking did not work, as the whole film contained Cu after the process and no emission in the visible could be detected from the exposed regions. This finding is in line with cross-linking of the carbon chain-based surface ligands as the underlying mechanism that protects the exposed regions from cation exchange.

In conclusion, we have developed a novel method to pattern NC films where the surface ligands function as a mask for a subsequent cation exchange process. This technique allows to

chemically transform selected regions of arbitrary shapes in an otherwise homogeneous NC film. The masked exchange process can be employed to fabricate luminescent patterns and electrical circuits in NC films without altering their morphology, adding new versatility to these materials. Next advances in this direction will explore the lateral resolution that can be achieved, which may critically depend on the choice of surface ligands on the NC surface, and their capability to undergo cross-linking that is sufficient to act as a barrier to cation exchange. Also processes that involve several cation exchange steps and therefore may enable the assembly of several different materials in a single film, are an interesting direction that will be explored. In a more mature state, the masked cation exchange technique has the potential to integrate miniaturized opto-electronic elements, for example on well-defined areas on a microchip, offering a possible disruptive technology for future integrated circuits.

■ ASSOCIATED CONTENT

S Supporting Information

Nanocrystal synthesis, optical properties of CdSe/CdS and $\text{Cu}_{2-x}\text{Se}/\text{Cu}_{2-x}\text{S}$ NCs, X-ray photoelectron spectroscopy, emission recorded before and after cation exchange from regions protected by e-beam and X-ray irradiation, mechanical response of the films by loading–unloading tests on both exposed and nonexposed regions on the samples, masked cation exchange in CdSe nanocrystal films, sequential cation exchange reactions on NC films after e-beam exposure. This material is available free of charge via the Internet at <http://pubs.acs.org>.

■ AUTHOR INFORMATION

Corresponding Authors

*E-mail: liberato.manna@iit.it.

*E-mail: roman.krahne@iit.it.

Author Contributions

K.M. and F.G. contributed equally to the work.

Notes

The authors declare no competing financial interest.

ACKNOWLEDGMENTS

We thank Francesco De Donato for providing the NC samples, Andrea Giugni for helpful discussions, and Gianluca Grenci for his assistance in the X-ray exposure experiments.

REFERENCES

- (1) Talapin, D. V.; Lee, J. S.; Kovalenko, M. V.; Shevchenko, E. V. *Chem. Rev.* **2010**, *110* (1), 389–458.
- (2) Vanmaekelbergh, D.; Liljeroth, P. *Chem. Soc. Rev.* **2005**, *34* (4), 299–312.
- (3) Luther, J. M.; Law, M.; Song, Q.; Perkins, C. L.; Beard, M. C.; Nozik, A. J. *ACS Nano* **2008**, *2* (2), 271–280.
- (4) Gao, Y.; Tang, Z. *Small* **2011**, *7* (15), 2133–2146.
- (5) Ye, X.; Chen, J.; Engel, M.; Millan, J. A.; Li, W.; Qi, L.; Xing, G.; Collins, J. E.; Kagan, C. R.; Li, J.; Glotzer, S. C.; Murray, C. B. *Nat. Chem.* **2013**, *5* (6), 466–473.
- (6) Dong, A.; Jiao, Y.; Milliron, D. J. *ACS Nano* **2013**, *7* (12), 10978–10984.
- (7) Sun, Y.; Rogers, J. A. *Adv. Mater.* **2007**, *19* (15), 1897–1916.
- (8) Nag, A.; Kovalenko, M. V.; Lee, J.-S.; Liu, W.; Spokoiny, B.; Talapin, D. V. *J. Am. Chem. Soc.* **2011**, *133* (27), 10612–10620.
- (9) Zhang, H.; Hu, B.; Sun, L.; Hovden, R.; Wise, F. W.; Muller, D. A.; Robinson, R. D. *Nano Lett.* **2011**, *11* (12), 5356–5361.
- (10) Kim, D. K.; Lai, Y.; Diroll, B. T.; Murray, C. B.; Kagan, C. R. *Nat. Commun.* **2012**, *3*, 1216.
- (11) Buonsanti, R.; Pick, T. E.; Krins, N.; Richardson, T. J.; Helms, B. A.; Milliron, D. J. *Nano Lett.* **2012**, *12* (7), 3872–3877.
- (12) Ip, A. H.; Thon, S. M.; Hoogland, S.; Voznyy, O.; Zhitomirsky, D.; Debnath, R.; Levina, L.; Rollny, L. R.; Carey, G. H.; Fischer, A.; Kemp, K. W.; Kramer, I. J.; Ning, Z.; Labelle, A. J.; Chou, K. W.; Amassian, A.; Sargent, E. H. *Nat. Nanotechnol.* **2012**, *7* (9), 577–582.
- (13) Tao, A. R.; Huang, J.; Yang, P. *Acc. Chem. Res.* **2008**, *41* (12), 1662–1673.
- (14) Cui, Y.; Bjork, M. T.; Liddle, J. A.; Sonnichsen, C.; Boussert, B.; Alivisatos, A. P. *Nano Lett.* **2004**, *4* (6), 1093–1098.
- (15) Thomas, P. J.; Kulkarni, G. U.; Rao, C. N. R. *J. Mater. Chem.* **2004**, *14* (4), 625–628.
- (16) Gundiah, G.; John, N. S.; Thomas, P. J.; Kulkarni, G. U.; Rao, C. N. R.; Heun, S. *Appl. Phys. Lett.* **2004**, *84* (26), 5341–5343.
- (17) Bodnarchuk, M. I.; Kovalenko, M. V.; Pichler, S.; Fritz-Popovski, G.; Hesser, G.; Heiss, W. *ACS Nano* **2010**, *4* (1), 423–431.
- (18) Tekin, E.; Smith, P. J.; Hoepfner, S.; Van Den Berg, A. M. J.; Susha, A. S.; Rogach, A. L.; Feldmann, J.; Schubert, U. S. *Adv. Funct. Mater.* **2007**, *17* (1), 23–28.
- (19) Kim, J. Y.; Ingrosso, C.; Fakhfouri, V.; Striccoli, M.; Agostiano, A.; Lucia Curri, M.; Brugger, J. *Small* **2009**, *5* (9), 1051–1057.
- (20) Mentzel, T. S.; Wanger, D. D.; Ray, N.; Walker, B. J.; Strasfeld, D.; Bawendi, M. G.; Kastner, M. A. *Nano Lett.* **2012**, *12* (8), 4404–4408.
- (21) Bedson, T. R.; Palmer, R. E.; Jenkins, T. E.; Hayton, D. J.; Wilcoxon, J. P. *Appl. Phys. Lett.* **2001**, *78* (13), 1921–1923.
- (22) Nandwana, V.; Subramani, C.; Yeh, Y. C.; Yang, B. Q.; Dickert, S.; Barnes, M. D.; Tuominen, M. T.; Rotello, V. M. *J. Mater. Chem.* **2011**, *21* (42), 16859–16862.
- (23) Plaza, J. L.; Chen, Y.; Jacke, S.; Palmer, R. E. *Langmuir* **2005**, *21* (4), 1556–1559.
- (24) Komarneni, M.; Shan, J.; Chakradhar, A.; Kadosssov, E.; Cabrini, S.; Burghaus, U. *J. Phys. Chem.* **2012**, *116* (9), 5792–5801.
- (25) Wu, Y.-T.; Liao, J.-D.; Weng, C.-C.; Hesieh, Y.-T.; Chen, C.-H.; Wang, M.-C.; Zharnikov, M. *J. Phys. Chem. C* **2009**, *113* (11), 4543–4548.
- (26) Zharnikov, M.; Grunze, M. *J. Vac. Sci. Technol., B* **2002**, *20* (5), 1793–1807.
- (27) Gadegaard, N.; Chen, X.; Rutten, F. J. M.; Alexander, M. R. *Langmuir* **2008**, *24* (5), 2057–2063.
- (28) Zharnikov, M.; Frey, S.; Heister, K.; Grunze, M. *Langmuir* **2000**, *16* (6), 2697–2705.
- (29) Son, D. H.; Hughes, S. M.; Yin, Y. D.; Alivisatos, A. P. *Science* **2004**, *306* (5698), 1009–1012.
- (30) Beberwyck, B. J.; Surendranath, Y.; Alivisatos, A. P. *J. Phys. Chem. C* **2013**, *117* (39), 19759–19770.
- (31) Rivest, J. B.; Jain, P. K. *Chem. Soc. Rev.* **2013**, *42* (1), 89–96.
- (32) Jain, P. K.; Amirav, L.; Aloni, S.; Alivisatos, A. P. *J. Am. Chem. Soc.* **2010**, *132* (29), 9997–9999.
- (33) Jain, P. K.; Beberwyck, B. J.; Fong, L.-K.; Polking, M. J.; Alivisatos, A. P. *Angew. Chem., Int. Ed.* **2012**, *51* (10), 2387–2390.
- (34) Robinson, R. D.; Sadler, B.; Demchenko, D. O.; Erdonmez, C. K.; Wang, L.-W.; Alivisatos, A. P. *Science* **2007**, *317* (5836), 355–358.
- (35) Rivest, J. B.; Swisher, S. L.; Fong, L.-K.; Zheng, H.; Alivisatos, A. P. *ACS Nano* **2011**, *5* (5), 3811–3816.
- (36) van Huis, M. A.; Young, N. P.; Pandraud, G.; Creemer, J. F.; Vanmaekelbergh, D.; Kirkland, A. I.; Zandbergen, H. W. *Adv. Mater.* **2009**, *21* (48), 4992–4995.
- (37) Zhang, H.; Solomon, L. V.; Ha, D. H.; Honrao, S.; Hennig, R. G.; Robinson, R. D. *Dalton Trans.* **2013**, *42* (35), 12596–12599.
- (38) Miszta, K.; Dorfs, D.; Genovese, A.; Kim, M. R.; Manna, L. *ACS Nano* **2011**, *5* (9), 7176–7183.
- (39) Ostermann, J.; Merkl, J.-P.; Flessau, S.; Wolter, C.; Kornowski, A.; Schmidtke, C.; Pietsch, A.; Kloust, H.; Feld, A.; Weller, H. *ACS Nano* **2013**, *7* (10), 9156–9167.
- (40) Sadler, B.; Demchenko, D. O.; Zheng, H.; Hughes, S. M.; Merkle, M. G.; Dahmen, U.; Wang, L.-W.; Alivisatos, A. P. *J. Am. Chem. Soc.* **2009**, *131* (14), 5285–5293.
- (41) Li, H.; Brescia, R.; Krahne, R.; Bertoni, G.; Alcocer, M. J. P.; D'Andrea, C.; Scotognella, F.; Tassone, F.; Zanella, M.; De Giorgi, M.; Manna, L. *ACS Nano* **2012**, *6* (2), 1637–1647.
- (42) Dilena, E.; Xie, Y.; Brescia, R.; Prato, M.; Maserati, L.; Krahne, R.; Paoletta, A.; Bertoni, G.; Povia, M.; Moreels, I.; Manna, L. *Chem. Mater.* **2013**, *25* (15), 3180–3187.
- (43) Carbone, L.; Nobile, C.; De Giorgi, M.; Sala, F. D.; Morello, G.; Pompa, P.; Hytch, M.; Snoeck, E.; Fiore, A.; Franchini, I. R.; Nadasan, M.; Silvestre, A. F.; Chiodo, L.; Kudera, S.; Cingolani, R.; Krahne, R.; Manna, L. *Nano Lett.* **2007**, *7* (10), 2942–2950.
- (44) Krahne, R.; Zavelani-Rossi, M.; Lupo, M. G.; Manna, L.; Lanzani, G. *Appl. Phys. Lett.* **2011**, *98* (6), No. 063105.
- (45) Kudera, S.; Zhang, Y.; Di Fabrizio, E.; Manna, L.; Krahne, R. *Phys. Rev. B* **2012**, *86* (7), No. 075307.
- (46) Hu, W.; Sarveswaran, K.; Lieberman, M.; Bernstein, G. H. *J. Vac. Sci. Technol., B* **2004**, *22* (4), 1711–1716.
- (47) Kaciulis, S. *Surf. Interface Anal.* **2012**, *44* (8), 1155–1161.
- (48) Turgeon, S.; Paynter, R. W. *Thin Solid Films* **2001**, *394* (1–2), 44–48.
- (49) Lesiak, B.; Zemek, J.; Houdkova, J.; Jiricek, P.; Józwik, A. *Polym. Degrad. Stab.* **2009**, *94* (10), 1714–1721.
- (50) Lee, D.; Jia, S.; Banerjee, S.; Bevk, J.; Herman, I. P.; Kysar, J. W. *Phys. Rev. Lett.* **2007**, *98* (2), No. 026103.
- (51) Podsiadlo, P.; Krylova, G.; Lee, B.; Critchley, K.; Gosztola, D. J.; Talapin, D. V.; Ashby, P. D.; Shevchenko, E. V. *J. Am. Chem. Soc.* **2010**, *132* (26), 8953–8960.
- (52) Yin, J.; Retsch, M.; Lee, J.-H.; Thomas, E. L.; Boyce, M. C. *Langmuir* **2011**, *27* (17), 10492–10500.
- (53) Falcaro, P.; Malfatti, L.; Vaccari, L.; Amenitsch, H.; Marmiroli, B.; Grenci, G.; Innocenzi, P. *Adv. Mater.* **2009**, *21* (48), 4932–4936.
- (54) Faustini, M.; Marmiroli, B.; Malfatti, L.; Louis, B.; Krins, N.; Falcaro, P.; Grenci, G.; Laberty-Robert, C.; Amenitsch, H.; Innocenzi, P.; Grossi, D. *J. Mater. Chem.* **2011**, *21* (11), 3597–3603.
- (55) Zhao, Y.; Pan, H.; Lou, Y.; Qiu, X.; Zhu, J.; Burda, C. *J. Am. Chem. Soc.* **2009**, *131* (12), 4253–4261.
- (56) Riha, S. C.; Johnson, D. C.; Prieto, A. L. *J. Am. Chem. Soc.* **2010**, *133* (5), 1383–1390.

- (57) Dorfs, D.; Haertling, T.; Miszta, K.; Bigall, N. C.; Kim, M. R.; Genovese, A.; Falqui, A.; Povia, M.; Manna, L. *J. Am. Chem. Soc.* **2011**, *133* (29), 11175–11180.
- (58) Luther, J. M.; Jain, P. K.; Ewers, T.; Alivisatos, A. P. *Nat. Mater.* **2011**, *10* (5), 361–366.
- (59) Paoletta, A.; George, C.; Povia, M.; Zhang, Y.; Krahne, R.; Gich, M.; Genovese, A.; Falqui, A.; Longobardi, M.; Guardia, P.; Pellegrino, T.; Manna, L. *Chem. Mater.* **2011**, *23* (16), 3762–3768.
- (60) Porter, V. J.; Mentzel, T.; Charpentier, S.; Kastner, M. A.; Bawendi, M. G. *Phys. Rev. B* **2006**, *73* (15), 155303.
- (61) Franchini, I. R.; Cola, A.; Rizzo, A.; Mastria, R.; Persano, A.; Krahne, R.; Genovese, A.; Falqui, A.; Baranov, D.; Gigli, G.; Manna, L. *Nanoscale* **2010**, *2* (10), 2171–2179.
- (62) Talapin, D. V.; Murray, C. B. *Science* **2005**, *310* (5745), 86–89.